

Triple Helicate—Tetrahedral Cluster Interconversion Controlled by Host–Guest Interactions**

Markus Scherer, Dana L. Caulder, Darren W. Johnson, and Kenneth N. Raymond*

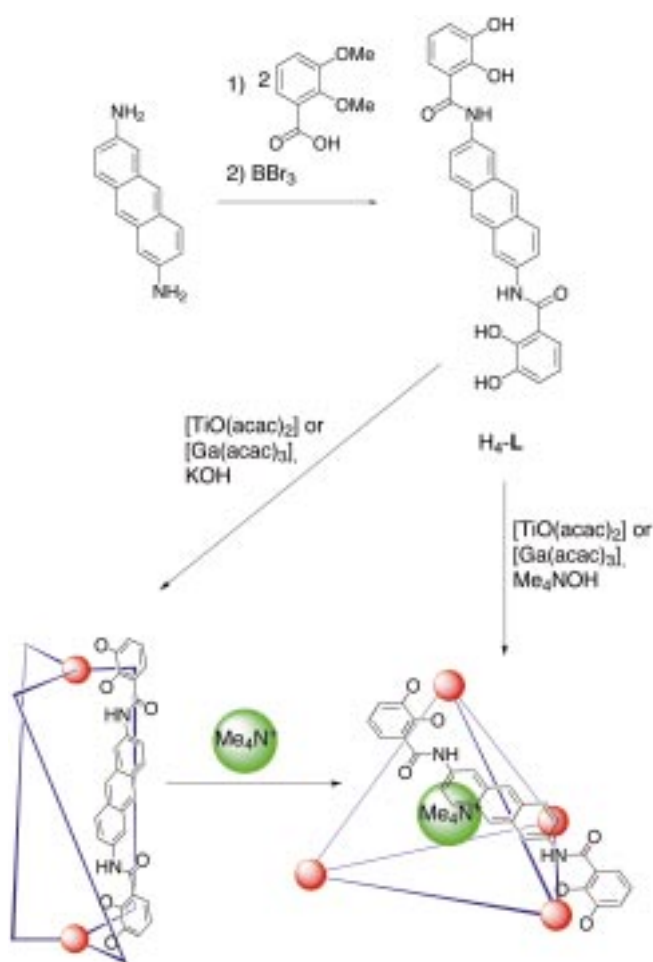
Dedicated to Professor Thomas Kruck on the occasion of his 65th birthday

Whereas natural clusters and synthetic analogues^[1] utilize hydrogen bonds and other numerous weak interactions, the use of stronger, highly directional, and well-studied metal–ligand interactions has recently provided many examples of clusters with a range of sizes, stoichiometries, and symmetries.^[2] We have recently demonstrated that a variety of high-symmetry coordination clusters can be rationally designed and synthesized in high-yield self-assembly reactions.^[3–12] Careful consideration of the geometric requirements of a particular symmetry and stoichiometry for a cluster can lead to the controlled formation of M_2L_3 triple helicates (D_3),^[8–10] M_4L_4 tetrahedra (T),^[7] and M_4L_6 tetrahedra (S_4 and T).^[6, 11]

Here we present an example of a bis(bidentate) catecholamide ligand whose geometry will allow for the formation of both an M_2L_3 triple helicate and an M_4L_6 tetrahedron. In the absence of a guest, an M_2L_3 triple helicate forms; however, in the presence of Me_4N^+ , the entropically disfavored M_4L_6 tetrahedron self-assembles to form a host–guest complex with Me_4N^+ encapsulated in the tetrahedral cluster cavity. Even more remarkably, the triple helicate can be quantitatively converted into the tetrahedron by addition of Me_4N^+ (Scheme 1).

The ligand H_4-L is based on a 2,6-diaminoanthracene backbone and is similar to a previously reported ligand system derived from 1,5-diaminonaphthalene.^[5, 6] For these types of backbones the catecholate binding units are offset when the ligand is in the conformation required to form a helicate, thus disfavoring helicate formation.^[13] Although the horizontal offset between the catecholate groups is exactly the same in both ligands, the extended length of H_4-L allows for greater flexibility in constructing the M_2L_3 structure.

Extensive molecular modeling of both the M_2L_3 and M_4L_6 structures was performed using the CAChe^[14] system (MM3) before beginning ligand synthesis. Results of these calculations indicated that both structures appeared equally plausible. These initial modeling investigations and the previous work with the 1,5-bis(2,3-dihydroxybenzamido)naphthalene



Scheme 1. Reaction of H_4-L with $[TiO(acac)_2]$ or $[Ga(acac)_3]$ leads to an M_2L_3 helicate in the absence of Me_4N^+ guest and an M_4L_6 tetrahedron in the presence of Me_4N^+ guest. The helicate can be converted into the tetrahedron simply by addition of Me_4N^+ .

ligand led us to believe that the M_2L_3 triple helicate structure could be formed by H_4-L , but that a strong host–guest interaction might push the equilibrium towards formation of the M_4L_6 tetrahedron.

Ligand H_4-L was synthesized according to established methods by coupling of 2,3-dimethoxybenzoyl chloride to 2,6-diaminoanthracene followed by deprotection with BBr_3 . Reaction of H_4-L (3 equiv), $[TiO(acac)_2]$ (2 equiv; $acac$ = acetylacetonate), and KOH (4 equiv) in methanol afforded after recrystallization orange microcrystals that analyze as $K_4[Ti_2-L_3] \cdot DMF \cdot 2H_2O$ (see Experimental Section). The highly symmetric 1H NMR spectrum exhibits downfield-shifted ligand resonances indicative of metal complex formation. Without high-resolution mass spectrometry results or a solid-state structure, however, there is no way to distinguish between a $K_4[Ti_2-L_3]$ or a $K_8[Ti_4-L_6]$ structure.^[15] Fortunately, the high-resolution electrospray mass spectrum shows that $K_4[Ti_2-L_3]$ does indeed form in solution.

A single-crystal X-ray diffraction study of this compound confirmed that the helicate structure is maintained in the solid state.^[16] The $[Ti_2-L_3]^{4-}$ tetraanion is a homochiral triple helicate ($\Delta\Delta$ or $\Lambda\Lambda$ at the metal centers) with a Ti–Ti distance of 16.7 Å (Figure 1). Disregarding the anthracene

[*] Prof. Dr. K. N. Raymond, Dr. M. Scherer, Dr. D. L. Caulder, D. W. Johnson
Department of Chemistry
University of California
Berkeley, CA 94720-1460 USA
Fax: (+1) 510-486-5283
E-mail: raymond@socrates.berkeley.edu

[**] Coordination Number Incommensurate Cluster Formation, Part 11. This research was supported by NSF grant CHE-9709621 and by exchange grants NSF INT-9603212 and NATO SRG951516. We thank the Alexander von Humboldt-Foundation for a fellowship to M.S. The authors gratefully acknowledge Dr. Fredrick J. Hollander for his assistance in solving the crystal structures, and the staff of the UC Berkeley Mass Spectrometry facility for their efforts in characterizing these clusters. Part 10: reference [10].

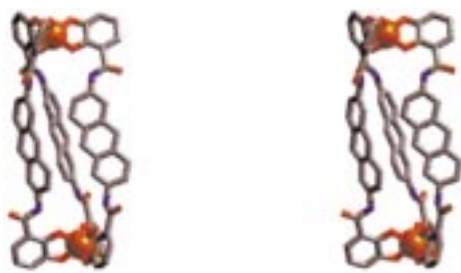


Figure 1. Stereoview of the crystal structure of $[\text{Ti}_2\text{-L}_3]^{4-}$.

backbones of the ligand, the tetraanion has approximately D_3 molecular symmetry. However, the threefold axis is lost because two of the anthracene rings are oriented with their edges directed into the cluster interior, while the third is oriented approximately perpendicular to the plane bisecting the angle between the two former anthracene ring planes. This third ligand is substantially nonplanar. Despite the anthracene ring (and all other aromatic rings) being restrained in the least-squares refinement to be flat, the deviations of the carbon atoms from the best-fit plane (RMS deviation 0.12) are significantly above the random deviations (RMS deviation 0.02–0.03) observed for the carbon atoms of the catechol rings and the remaining two anthracene rings. In addition to this bend of the anthracene ring, the nitrogen atoms of the amide moieties show even greater deviation (≈ 0.25 Å) from the anthracene least-squares plane. In effect, this ligand is bowed *out* from the cluster interior.

In each of the three ligands, the catechol rings are not coplanar with the anthracene backbone. The angles between the least squares planes calculated for the catechol rings and the anthracene backbone are $61.0(0.6)^\circ$ and $18.0(1.0)^\circ$ for the first ligand, $44.9(0.6)^\circ$ and $6.6(1.1)^\circ$ for the second ligand, and $72.4(0.7)^\circ$ and $44.9(0.8)^\circ$ for the third ligand. The third ligand, which shows the most substantial twisting about the amide N–C bond, is the one previously described as being curved.

It is apparent from the crystal structure that this particular ligand allows for the formation of the M_2L_3 structure, but “just barely.” The third ligand shows substantial strain, as evidenced by the curvature of the aromatic backbone and the twists of the catechol rings with respect to the anthracene backbone. The ideal symmetry of a triple helicate (D_3), therefore, is not possible. As mentioned above, the ^1H NMR spectrum of $\text{K}_4[\text{Ti}_2\text{-L}_3]$ shows a single high-symmetry product on the NMR timescale. Variable-temperature NMR experiments are underway to determine if the asymmetry seen in the solid-state structure can also be observed at low temperature in solution.

Previous results suggested that alkylammonium cations might be suitable guests for the proposed tetrahedral cluster host.^[5, 6] Reaction of $\text{H}_4\text{-L}$ (3 equiv), $[\text{TiO}(\text{acac})_2]$ (2 equiv), and Me_4NOH (4 equiv) in methanol leads to an orange precipitate that analyzes as $[\text{Me}_4\text{N}]_8[\text{Ti}_4\text{-L}_6] \cdot 3\text{DMF} \cdot \text{H}_2\text{O}$. The ^1H NMR spectrum of this product shows a single, highly symmetric product with two Me_4N^+ resonances in a ratio of 7:1 ($\delta = 3.97, -2.60$). The presence of the extremely upfield shifted Me_4N^+ resonance ($\delta = -2.6$) whose relative intensity corresponds to one Me_4N^+ cation to six ligands can be interpreted as a direct indication of the encapsulation of one

Me_4N^+ cation by the tetrahedral cluster $[\text{Ti}_4\text{-L}_6]^{8-}$.^[6, 7, 17] In turn, this encapsulation indicates successful formation of the tetrahedral cluster.

^{13}C NMR spectroscopy and high-resolution electrospray mass spectrometry results support the assignment of this species in solution as the $[\text{Ti}_4\text{-L}_6]^{8-}$ cluster. Two resonances ($\delta = 54.54, 49.32$) for the Me_4N^+ cation are observed in the ^{13}C NMR spectrum. In the ES mass spectrum all peaks can be assigned to the tetrahedral $[\text{Ti}_4\text{-L}_6]^{8-}$ cluster; these peaks are for the compositions $[\text{Me}_4\text{N}^+]_n[\text{Ti}_4\text{-L}_6]^{(8-n)-}$ ($n = 2-6$) and $\text{H}_m[\text{Me}_4\text{N}^+]_n[\text{Ti}_4\text{-L}_6]^{(8-m-n)-}$ ($m = 1, n = 3-4; m = 2, n = 0, 2, 3$). Due to the high resolution of the results from the experiment, the charge states of all the signals (except those with 6 – charge) were confirmed by inspection of the peak separations. For example, the signal for $[\text{Me}_4\text{N}^+]_5[\text{Ti}_4\text{-L}_6]^{3-}$ at m/z 1140.4 has a peak separation of 0.3 amu, indicative of a 3 – charge state.

A single-crystal X-ray diffraction study of this compound confirmed that the tetrahedral structure is maintained in the solid state.^[18] Crystallographic analysis of $(\text{Me}_4\text{N})_8[\text{Ti}_4\text{-L}_6] \cdot 4\text{H}_2\text{O} \cdot 2\text{DMF} \cdot 2\text{C}_4\text{H}_8\text{O}_2 \cdot x\text{solvent}$ showed it to be a high-symmetry cluster in which the four Ti^{IV} ions are in a tetrahedral array bridged by six ligands (Figure 2). The octaanion is a racemic mixture of homochiral tetrahedra ($\Delta\Delta\Delta\Delta$ or $\Lambda\Lambda\Lambda\Lambda$ at the metal centers) with an average Ti–Ti distance of 16.1 Å. Additionally, a Me_4N^+ cation was found encapsulated within the cavity of this cluster.

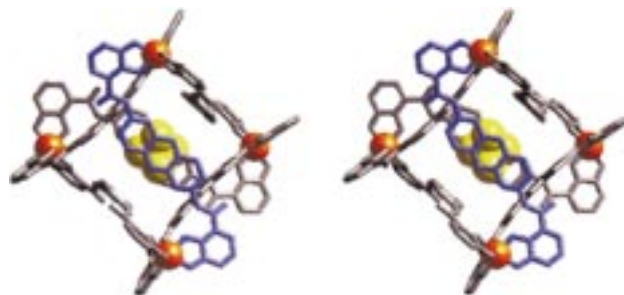


Figure 2. Stereoview of the crystal structure of $\text{Me}_4\text{N}^+ \subset [\text{Ti}_4\text{-L}_6]^{8-}$.

The tetranuclear complex has crystallographic D_2 symmetry and idealized T symmetry. There is little twisting about the amide moiety in the tetrahedral cluster as compared to the helicate; the angles between the least-squares planes calculated for the anthracene and catecholate rings range from only 9.4° to 12.7° . The ligands are, however, bowed in towards the cavity, presumably in order to make van der Waals contact with the small Me_4N^+ cation. The deviations of the carbon atoms of the anthracene rings from the best-fit planes (RMS deviation 0.11 Å) are significantly above the random deviations (RMS deviation 0.03–0.04 Å) observed for the carbon atoms of the catechol rings. In addition to this bend of the anthracene rings, the nitrogen atoms of the amide moieties show even greater deviation (≈ 0.29 Å) from the anthracene least-squares planes. Furthermore, in the tetrahedron the catechol binding units of each ligand are pointed in towards one another (antiparallel coordinate vectors); in the helicate the ligands are contorted to allow the two catecholate binding units of each ligand to align in roughly the same direction (parallel coordinate vectors). This represents an elegant proof

of principle for our rational design of these two types of systems.^[13]

Since the only difference in the two systems described is the absence or presence of Me_4N^+ , it should be possible to transform a triple helicate into a tetrahedral cluster simply by addition of Me_4N^+ . To test this hypothesis, the gallium(III) analogues were prepared because of the greater lability of Ga^{III} compared to Ti^{IV} . Upon addition of 20 equivalents of Me_4NCl to a solution of $\text{K}_6[\text{Ga}_2\text{-L}_3]$ in D_2O , complete transformation of the helicate into the tetrahedral cluster occurred. This was monitored by ^1H NMR spectroscopy over the course of five days (pD 6.5, $T = 40^\circ\text{C}$; Figure 3). Similar transformation studies at higher pD values (pD 7.5) and lower temperatures (room temperature) resulted in lower conversion rates due to the slower kinetics of metal–ligand rearrangement under these conditions.

In summary, we have shown that two different clusters, a triple helicate and a tetrahedron, can be prepared using identical ligand and metal components.^[19–22] Both structures conform to the rational design we have proposed for such clusters, and the relative energies are consistent with model predictions. Simply the addition of an appropriate guest is enough to shift the equilibrium from the entropically preferred helicate to the tetrahedron. More remarkably, the triple helicate can be quantitatively transformed into the tetrahedron by simple addition of this guest, Me_4N^+ . While we have demonstrated control of cluster synthesis by control of ligand geometry, these results show that we can also systematically use host–guest interactions in the rational design and synthesis of supramolecular clusters.

Experimental Section

General: All NMR spectra were measured with a Bruker 500-MHz spectrometer. Chemical shifts are reported as in ppm downfield from tetramethylsilane (TMS).

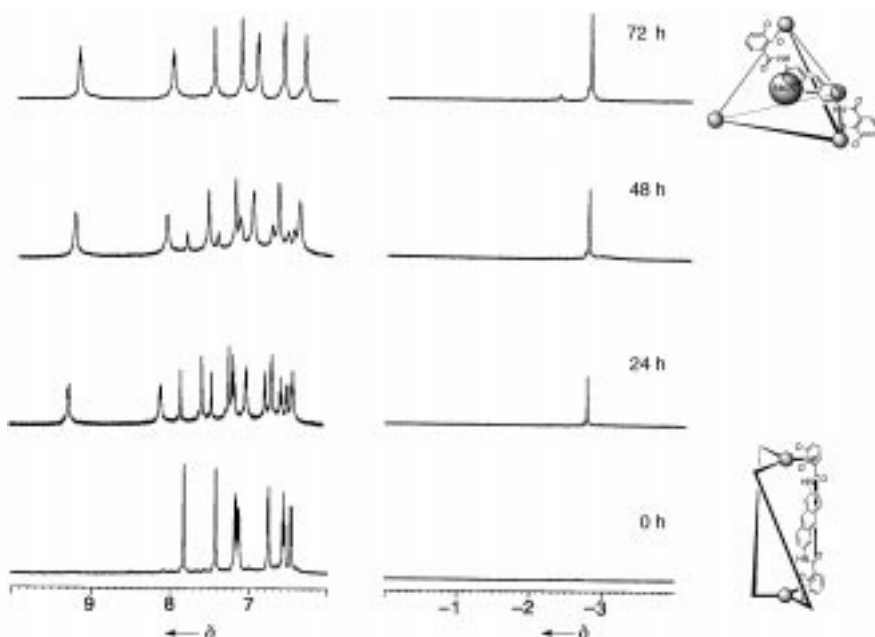


Figure 3. ^1H NMR spectra of helicate–tetrahedral cluster interconversion (D_2O , pD 6.5). Addition of Me_4N^+ to a solution of $\text{K}_6[\text{Ga}_2\text{-L}_3]$ leads to quantitative transformation of $\text{Me}_4\text{N}^+ \subset [\text{Ga}_4\text{-L}_6]^{12-}$.

$\text{Me}_4\text{-L}$: Under a N_2 atmosphere, 2,6-diaminoanthracene^[23] (706 mg, 3.4 mmol) was added all at once to 2,3-dimethoxybenzoyl chloride^[24] (1.36 g, 6.78 mmol) in dry CH_2Cl_2 (60 mL) followed by the addition of excess Et_3N (1.5 mL). The mixture was stirred for 20 h and then successively washed with 1N HCl, 10% aq NaOH, and brine. After drying of the solution over MgSO_4 and removal of the solvent under vacuum, a yellow powder was obtained. The product was further purified by layering a solution of the powder in CHCl_3 with Et_2O to yield yellow microcrystals (0.78 g, 43%). ^1H NMR (500 MHz, $[\text{D}_6]\text{DMSO}$): $\delta = 10.47$ (s, 2H), 8.62 (s, 2H), 8.42 (s, 2H), 8.02 (d, 2H), 7.64 (d, 2H), 7.19 (m, 6H), 3.85 (d, 12H); ^{13}C NMR (125 MHz, $[\text{D}_6]\text{DMSO}$): $\delta = 166.55$, 153.87, 136.45, 132.15, 131.89, 129.93, 129.18, 125.75, 124.96, 122.13, 121.26, 121.15, 115.46, 112.76; 62.06, 56.78; FAB-MS (positive ion): m/z : 537 (MH^+ , 100%); elemental analysis calcd (found) for $\text{C}_{32}\text{H}_{28}\text{N}_2\text{O}_6 \cdot 1.5\text{H}_2\text{O}$: C 68.19 (68.25), H 5.54 (5.52), N 4.97 (5.01).

$\text{H}_4\text{-L}$: Boron tribromide (1.25 mL, 12.2 mmol) was added by syringe to a N_2 -purged solution of $\text{Me}_4\text{-L}$ (0.37 g, 0.77 mmol) in dry CH_2Cl_2 at -78°C . The mixture was allowed to warm to room temperature and was stirred overnight under a N_2 atmosphere. The volatile components were removed under vacuum, and the resulting solid was hydrolyzed with water and stirred for 2 h at 100°C . The yellow-green solid was collected by filtration, washed with water and Et_2O , and dried under vacuum (0.32 g, 93%). ^1H NMR (500 MHz, $[\text{D}_6]\text{DMSO}$): $\delta = 11.61$ (brs, 2H), 10.57 (s, 2H), 9.47 (brs, 2H), 8.53 (s, 2H), 8.48 (s, 2H), 8.08 (d, 2H), 7.72 (d, 2H), 7.49 (d, 2H), 7.00 (d, 2H), 6.80 (t, 2H); ^{13}C NMR (125 MHz, $[\text{D}_6]\text{DMSO}$): $\delta = 168.25$, 148.57, 146.62, 135.25, 131.29, 129.74, 128.88, 125.74, 122.70, 119.45, 118.99, 118.94, 117.77, 117.17; FAB-MS (positive ion): m/z : 481 (MH^+ , 100%); elemental analysis calcd (found) for $\text{C}_{28}\text{H}_{20}\text{N}_2\text{O}_6 \cdot 4\text{H}_2\text{O}$: C 60.87 (60.93), H 5.11 (5.07), N 5.07 (5.04).

$\text{K}_4[\text{Ti}_2\text{-L}_3]$: The ligand $\text{H}_4\text{-L}$ (150 mg, 0.312 mmol) was suspended under oxygen-free conditions in CH_3OH (30 mL). A 0.508N KOH solution in CH_3OH (817 μL) was added by a pipetteman. $[\text{TiO}(\text{acac})_2]$ (55 mg, 0.21 mmol) was added as a powder, after which the solution gradually turned orange. The mixture was stirred overnight, and the solvent subsequently removed under vacuum to afford a red solid, which was purified by recrystallization from DMF/ Et_2O (156 mg; 89%). Crystals suitable for analysis by X-ray diffraction were obtained by the slow vapor diffusion of Et_2O into a solution of the complex in DMF/THF. ^1H NMR (500 MHz, $[\text{D}_6]\text{DMSO}$): $\delta = 11.66$ (s, 6H), 8.01 (s, 6H), 7.68 (s, 6H), 7.30 (d, 6H), 7.15 (d, 6H), 7.13 (d, 6H), 6.50 (t, 6H), 6.39 (d, 6H); ^{13}C NMR (125 MHz, $[\text{D}_6]\text{DMSO}$): $\delta = 165.25$, 161.11, 160.09, 135.45, 132.09, 129.16, 129.13, 125.04, 122.78, 117.78, 117.05, 116.96, 115.33, 113.89; ESI-MS (positive ion): m/z : 1567.3 ($\text{H}_4\text{K}[\text{Ti}_2\text{-L}_3]^+$, 97%), 1529.4 ($\text{H}_3[\text{Ti}_2\text{-L}_3]^+$, 83%), 765.2 ($\text{H}_6[\text{Ti}_2\text{-L}_3]^{2+}$, 100%); elemental analysis calcd (found) for $\text{K}_4[\text{Ti}_2\text{-L}_3] \cdot \text{DMF} \cdot 2\text{H}_2\text{O}$: C 58.84 (58.76), H 3.32 (3.25), N 5.48 (5.41).

$\text{K}_6[\text{Ga}_2\text{-L}_3]$: Prepared as above using $[\text{Ga}(\text{acac})_3]$. The product was recrystallized by layering a solution in CH_3OH with Et_2O (98%). ^1H NMR (500 MHz, $[\text{D}_4]\text{MeOH}$): $\delta = 8.01$ (d, 6H), 7.39 (d, 6H), 7.17 (d, 6H), 7.11 (d, 6H), 6.87 (d, 6H), 6.73 (d, 6H), 6.42 (t, 6H); ^{13}C NMR (125 MHz, $[\text{D}_6]\text{DMSO}$): $\delta = 164.65$, 161.06, 160.01, 134.45, 131.38, 129.01, 128.89, 125.01, 122.28, 117.18, 117.06, 116.98, 115.31, 113.22; ESI-MS (positive ion): m/z : 1576 ($\text{H}_7[\text{Ga}_2\text{-L}_3]^+$, 100%); elemental analysis calcd (found) for $\text{K}_4[\text{Ga}_2\text{-L}_3] \cdot \text{DMF}$: C 55.69 (55.76), H 2.95 (2.89), N 5.26 (5.28).

$(\text{Me}_4\text{N})_8[\text{Ti}_4\text{-L}_6]$: Prepared as above using $[\text{TiO}(\text{acac})_2]$ and Me_4NOH instead of KOH. The orange precipitate was collected by filtration and recrystallized by layering a solution in DMF with Et_2O (73 mg, 61%). Single crystals suitable for X-ray diffraction were grown by the slow vapor diffusion of ethyl acetate into a wet solution of the complex in DMF. ^1H NMR (500 MHz, $[\text{D}_6]\text{DMSO}$): $\delta = 14.79$ (s, 12H), 9.47 (d, 12H), 7.86 (d, 12H), 7.49 (s, 12H), 7.29 (s, 12H), 6.79 (d,

12H), 6.32 (d, 12H), 6.23 (t, 12H), 3.97 (s, 84H), -2.55 (12H); ^{13}C NMR (125 MHz, $[\text{D}_6]\text{DMSO}$): $\delta = 168.34, 159.94, 157.98, 138.94, 130.35, 128.39, 127.81, 123.01, 122.03, 113.95, 112.87, 112.73, 112.31, 112.12; 54.54, 49.32$; ESI-MS (negative ion): m/z : 1747.2 ($(\text{Me}_4\text{N})_6[\text{Ti}_4\text{-L}_6]^{2-}$), 1140.4 ($(\text{Me}_4\text{N})_5[\text{Ti}_4\text{-L}_6]^{3-}$), 1116.0 ($(\text{H}(\text{Me}_4\text{N})_4[\text{Ti}_4\text{-L}_6]^{3-})$), 1091.7 ($(\text{H}_2(\text{Me}_4\text{N})_3[\text{Ti}_4\text{-L}_6]^{3-})$), 818.3 ($(\text{H}(\text{Me}_4\text{N})_3[\text{Ti}_4\text{-L}_6]^{4-})$), 836.8 ($(\text{Me}_4\text{N})_4[\text{Ti}_4\text{-L}_6]^{4-}$, 100%), 800.6 ($(\text{H}_2(\text{Me}_4\text{N})_2[\text{Ti}_4\text{-L}_6]^{4-})$), 654.4 ($(\text{Me}_4\text{N})_3[\text{Ti}_4\text{-L}_6]^{5-}$), 533.4 ($(\text{Me}_4\text{N})_2[\text{Ti}_4\text{-L}_6]^{6-}$), 509.1 ($(\text{H}_2[\text{Ti}_4\text{-L}_6]^{6-})$); elemental analysis calcd (found) for $[\text{Me}_4\text{N}]_8[\text{Ti}_4\text{-L}_6] \cdot 3\text{DMF} \cdot 2\text{H}_2\text{O}$: C 64.39 (64.46), H 5.61 (5.56), N 8.26 (8.32).

$\text{K}_4(\text{Me}_4\text{N})_8[\text{Ga}_4\text{-L}_6]$: Prepared as above using $[\text{Ga}(\text{acac})_3]$, KOH, and Me_4NCl . The product was precipitated by reducing the volume of the solution slowly to 5 ml. The yellow precipitate was collected by filtration and dried under high vacuum (61 mg, 91%). ^1H NMR (500 MHz, $[\text{D}_6]\text{DMSO}$): $\delta = 14.79$ (s, 12H), 9.39 (d, 12H), 7.81 (d, 12H), 7.46 (s, 12H), 7.21 (s, 12H), 6.78 (d, 12H), 6.26 (d, 12H), 6.08 (t, 12H), 3.95 (s, 84H), -2.60 (s, 12H); ^{13}C NMR (125 MHz, $[\text{D}_6]\text{DMSO}$): $\delta = 167.88, 159.67, 157.60, 138.56, 130.04, 127.89, 127.81, 123.01, 122.03, 113.95, 112.87, 112.73, 112.31, 112.02, 54.70, 49.97$.

Received: November 27, 1998 [Z 12722 IE]

German version: *Angew. Chem.* **1999**, *111*, 1690–1694

Keywords: cage compounds • cluster compounds • helical structures • host–guest chemistry • supramolecular chemistry

- [1] For examples see M. M. Conn, J. J. Rebek, *Chem. Rev.* **1997**, *97*, 1647–1668.
- [2] See examples in a) J.-M. Lehn, *Supramolecular Chemistry: Concepts and Perspectives*, VCH, Weinheim, **1995**; b) D. S. Lawrence, T. Jiang, M. Levett, *Chem. Rev.* **1995**, *95*, 2229–2260; c) C. Piquet, G. Bernardinelli, G. Hopfgartner, *Chem. Rev.* **1997**, *97*, 2005–2062; d) B. Linton, A. D. Hamilton, *Chem. Rev.* **1997**, *97*, 1669–1680; e) P. J. Stang, *Chem. Eur. J.* **1998**, *4*, 19–27.
- [3] D. L. Caulder, K. N. Raymond, *J. Chem. Soc. Dalton Trans.* **1999**, 1185–1200.
- [4] X. Sun, D. W. Johnson, D. L. Caulder, R. E. Powers, K. N. Raymond, E. H. Wong, *Angew. Chem.* **1999**, 1386–1390; *Angew. Chem. Int. Ed.* **1999**, 1303–1307.
- [5] T. Parac, D. L. Caulder, K. N. Raymond, *J. Am. Chem. Soc.* **1998**, *120*, 8003–8004.
- [6] D. L. Caulder, R. E. Powers, T. Parac, K. N. Raymond, *Angew. Chem.* **1998**, *110*, 1940–1943; *Angew. Chem. Int. Ed.* **1998**, *37*, 1840–1843.
- [7] C. Brückner, R. E. Powers, K. N. Raymond, *Angew. Chem.* **1998**, *110*, 1937–1940; *Angew. Chem. Int. Ed.* **1998**, *37*, 1837–1839.
- [8] a) M. Meyer, B. Kersting, R. E. Powers, K. N. Raymond, *Inorg. Chem.* **1997**, *36*, 5179–5191; b) B. Kersting, M. Meyer, R. E. Powers, K. N. Raymond, *J. Am. Chem. Soc.* **1996**, *118*, 7221.
- [9] D. L. Caulder, K. N. Raymond, *Angew. Chem.* **1997**, *109*, 1508–1510; *Angew. Chem. Int. Ed. Engl.* **1997**, *36*, 1439–1442.
- [10] J. Xu, T. N. Parac, K. N. Raymond, *Angew. Chem.* **1999**, in press; *Angew. Chem. Int. Ed.* **1999**, in press.
- [11] T. Beissel, R. E. Powers, K. N. Raymond, *Angew. Chem.* **1996**, *108*, 1166; *Angew. Chem. Int. Ed. Engl.* **1996**, *35*, 1084–1086.
- [12] K. N. Raymond, D. L. Caulder, R. E. Powers, T. Beissel, M. Meyer, B. Kersting, *Chem. Res.* **1996**, *40*, 115–129 (*Proc. 40th Robert A. Welch Found.*).
- [13] The parallel coordinate vectors of the catecholate binding groups must point in the same direction to form a helicate and in opposite directions to form a tetrahedron.
- [14] CAChe, 4.0, **1997**, Oxford Molecular Group, Inc., USA.
- [15] Such characterization requires mass spectrometry or crystallographic characterization.
- [16] Crystal data for $\text{K}_4[\text{Ti}_2\text{-L}_3] \cdot 8\text{DMF}$: The data were collected using a Siemens SMART diffractometer equipped with a CCD area detector;^[25] crystal size $0.25 \times 0.16 \times 0.12$ mm; $T = -146^\circ\text{C}$, graphite-monochromated MoK_α radiation ($\lambda = 0.71073$ Å); monoclinic, space group *Cc* (no. 9), $a = 49.6848(13)$, $b = 11.9175(3)$, $c = 22.0824(6)$ Å, $\beta = 113.571(1)^\circ$, $V = 11984.5(5)$ Å³, $Z = 4$, $\mu = 0.345$ mm⁻¹, $F(000) = 4712$, $\rho_{\text{calcd}} = 1.256$ Mg m⁻³, $2\theta_{\text{max}} = 37.7^\circ$. The data were integrated using SAINT.^[26] Of the 23943 reflections collected, 13861 were Friedel unique ($R_{\text{int}} = 0.0753$). The structure was solved by direct methods and refined on F^2 using SHELXTL.^[27] Data were corrected for Lorentz and polarization effects. Outliers with $\Delta I/\sigma > 5$ ($\Delta I/\sigma > 10$ if only two equivalents) were rejected, resulting in 224 reflections (0.90% of the data) being removed. An empirical absorption correction was applied using SADABS^[28] (ellipsoidal model, $T_{\text{max}} = 0.928$, $T_{\text{min}} = 0.750$). The structure was modeled as a racemic twin (50:50) in the non-centrosymmetric space group *Cc* (no. 9).^[29] Inspection shows that the cluster does actually crystallize in the non-centrosymmetric space group *Cc*, not its centrosymmetric counterpart *C2/c*. The twofold axis that would run through the cluster is only approximate: The ligand that would be perpendicular to this twofold axis is significantly distorted from twofold symmetry. The catecholate rings and the anthracene ring are offset from the would-be symmetry axis. The lack of high-angle data resulted in a low-resolution (1.1 Å) structure that necessitated the use of numerous restraints. Weighting scheme: $1/[\sigma^2(F_o^2) + (0.2911p)^2 + 74.6955p]$, where $p = (F_o^2 + 2F_c^2)/3$. Final $R1 = 0.1468$ for 7925 Friedel unique data (767 parameters, 487 restraints, $2.72^\circ < 2\theta < 37.7^\circ$); for all 13861 data, $wR_2 = 0.4780$, $\text{GOF} = 1.103$; max./min. residual density $+1.553/-0.606$ e Å⁻³ (the largest difference peak was located 0.82 Å from Ti1 between the two coordinating catechol oxygen atoms).^[18b]
- [17] a) P. Jacopozi, E. Dalcanele, *Angew. Chem.* **1997**, *109*, 665–667; *Angew. Chem. Int. Ed. Engl.* **1997**, *36*, 613–615; b) S. Mann, G. Huttner, L. Zsolnai, K. Heinze, *Angew. Chem.* **1996**, *108*, 2983–2984; *Angew. Chem. Int. Ed. Engl.* **1996**, *35*, 2808–2809; c) M. Fujita, D. Oguro, M. Miyazawa, H. Oka, K. Yamaguchi, K. Ogura, *Nature* **1995**, *378*, 469–471; d) J. S. Fleming, K. L. V. Mann, C.-A. Carraz, E. Psillakis, J. C. Jeffery, J. A. McCleverty, M. D. Ward, *Angew. Chem.* **1998**, *110*, 1315–1318; *Angew. Chem. Int. Ed.* **1998**, *37*, 1279–1281; e) J. Bryant, M. T. Blanda, M. Vincenti, D. J. Cram, *J. Am. Chem. Soc.* **1991**, *113*, 2167–2172; f) P. Timmerman, W. Verboom, F. C. J. M. van Veggel, J. P. M. van Duynhoven, D. N. Reinhoudt, *Angew. Chem.* **1994**, *106*, 2437–2440; *Angew. Chem. Int. Ed. Engl.* **1994**, *33*, 2345–2348.
- [18] a) Crystal data for $(\text{Me}_4\text{N})_8[\text{Ti}_4\text{-L}_6] \cdot 4\text{H}_2\text{O} \cdot 2\text{DMF} \cdot 2\text{C}_4\text{H}_9\text{O}_2 \cdot x\text{solvent}$: The data were collected using a Siemens SMART diffractometer equipped with a CCD area detector;^[25] crystal size $0.16 \times 0.12 \times 0.12$ mm; $T = -134^\circ\text{C}$, graphite-monochromated MoK_α radiation ($\lambda = 0.71073$ Å); tetragonal, space group *P4/ncc* (no. 130), $a = 26.5931(6)$, $c = 33.5365(12)$ Å, $V = 23717(1)$ Å³, $Z = 4$, $\mu = 0.212$ mm⁻¹, $F(000) = 9300$, $\rho_{\text{calcd}} = 1.247$ Mg m⁻³, $2\theta_{\text{max}} = 30.52^\circ$. Of the 34354 reflections collected, 2526 were unique ($R_{\text{int}} = 0.1417$). The data were integrated using SAINT.^[26] The structure was solved by direct methods using teXsan^[30] and refined on F^2 using SHELXTL.^[27] Data were corrected for Lorentz and polarization effects. An empirical absorption correction was applied using SADABS^[28] (ellipsoidal model, $T_{\text{max}} = 0.887$, $T_{\text{min}} = 0.834$). The lack of high-angle data resulted in a low-resolution (1.35 Å) structure that necessitated the use of numerous restraints. Weighting scheme: $1/[\sigma^2(F_o^2) + (0.1000p)^2]$, where $p = (F_o^2 + 2F_c^2)/3$. Final $R1 = 0.1748$ for 1826 with $I > 2\sigma(I)$ (398 parameters, 193 restraints, $2.16^\circ < 2\theta < 30.48^\circ$); for all 2526 data, $wR_2 = 0.4189$, $\text{GOF} = 3.021$; max./min. residual density $+2.210/-0.393$ e Å⁻³. The largest difference peaks correspond to noise near the special positions. b) Crystallographic data (excluding structure factors) for the structures reported in this paper have been deposited with the Cambridge Crystallographic Data Center as supplementary publication no. CCDC-101878 (helicate) and CCDC-109439 (tetrahedron). Copies of the data can be obtained free of charge on application to CCDC, 12 Union Road, Cambridge CB2 1EZ, UK (fax: (+44) 1223-336-033; e-mail: deposit@ccdc.cam.ac.uk).
- [19] For an example in which interaction with a counteranion can change cluster stoichiometry and geometry, see a) B. Hasenknopf, J.-M. Lehn, N. Boumediene, A. Dupont-Gervais, A. Van Dorsselaer, B. Kneisel, D. Fenske, *J. Am. Chem. Soc.* **1997**, *119*, 10956–10962; b) B. Hasenknopf, J.-M. Lehn, B. O. Kneisel, G. Baum, D. Fenske, *Angew. Chem.* **1996**, *108*, 1987–1990; *Angew. Chem. Int. Ed. Engl.* **1996**, *35*, 1838–1840.

- [20] For an example of a system in which the use of different metal ions leads to changes in cluster stoichiometry and geometry, see reference [17d].
- [21] For examples of systems in which slight structural modifications in the ligand changes cluster stoichiometry and geometry, see a) C. Provent, S. Hewage, G. Brand, G. Bernardinelli, L. J. Charbonnière, A. F. Williams, *Angew. Chem.* **1997**, *109*, 1346–1348; *Angew. Chem. Int. Ed. Engl.* **1997**, *36*, 1287–1289; b) E. J. Enemark, T. D. P. Stack, *Angew. Chem.* **1998**, *110*, 977–981; *Angew. Chem. Int. Ed.* **1998**, *37*, 932–935.
- [22] For examples of solutions containing mixtures of clusters with different stoichiometry and geometry, see a) F. M. Romero, R. Ziessel, A. Dupont-Gervais, A. Van Dorsselaer, *Chem. Commun.* **1996**, 551–553; b) P. N. W. Baxter, J.-M. Lehn, *Chem. Commun.* **1997**, 1323–1324.
- [23] A slightly modified preparation (using SnCl_2) based on a literature procedure (M. A. Rabjohns, P. Hodge, P. A. Lovell, *Polymer* **1997**, *38*, 3395–3407) was used.
- [24] P. F. Schuda, C. M. Botti, M. C. Venuti, *OPPI Briefs* **1984**, *16*, 119–123.
- [25] SMART, Area Detector Software Package, **1995**, Siemens Industrial Automation, Inc., Madison, WI, USA.
- [26] SAINT, SAX Area Detector Integration Program, 4.024, **1995**, Siemens Industrial Automation, Inc., Madison, WI, USA.
- [27] G. Sheldrick, SHELXTL Crystal Structure Determination Software Package, **1993**, Siemens Industrial Automation, Inc., Madison, WI, USA.
- [28] G. Sheldrick, SADABS, Siemens Area Detector ABSorption Correction Program, Advanced Copy, **1996**; G. Sheldrick, personal communication.
- [29] C. S. Pratt, B. A. Coyle, J. A. Ibers, *J. Chem. Soc. A* **1971**, 2146–2151.
- [30] teXsan, Crystal Structure Analysis Package, **1992**, Molecular Structure Corporation, The Woodlands, TX, USA.

A Simple Lithographic Approach for Preparing Patterned, Micron-Scale Corrals for Controlling Cell Growth**

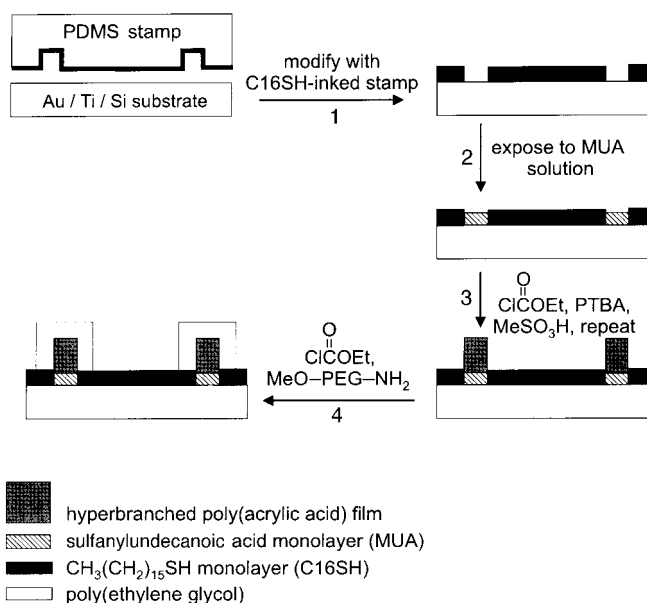
Pradyut Ghosh, Mary Lee Amirpour, William M. Lackowski, Michael V. Pishko, and Richard M. Crooks*

In this report we demonstrate that a simple, three-step lithographic process—involving microcontact printing ($\mu\text{-CP}$), polymer grafting, and subsequent polymer functionalization—results in patterned surfaces exhibiting excellent cell

adhesion and spatial definition. The patterned substrates consist of cell corrals having lateral dimensions of $63\ \mu\text{m}$ and wall heights of $54 \pm 4\ \text{nm}$. The corrals have hydrophobic, methyl-terminated *n*-alkanethiolate bottoms, which promote cell adhesion, and the walls consist of hydrophilic poly(acrylic acid)/poly(ethylene glycol) (3-PAA/PEG) nanocomposite polymers that resist cell encroachment. Peritoneal IC-21 murine macrophage cell growth occurs only within the boundaries of the corrals. This approach provides a simple and chemically flexible route to local definition of cells on surfaces.

Formation of biological tissue structures, such as nerves and blood vessels, require micron-scale morphologic control and spatial positioning of cells. To achieve this on artificial substrates, the adsorption and adhesion of cells and proteins have been studied on self-assembled monolayers (SAMs) made up of alkanethiolates or alkylsilanes and on thin polymer films.^[1–5] There have been a smaller number of studies focused on the adhesion and motility of cells on patterned substrates.^[6–11]

Our approach for exerting micron-scale control over cell adhesion involves four steps (Scheme 1).^[12] After preparation of a suitable poly(dimethylsiloxane) (PDMS) stamp from a TEM-grid master (TEM = transmission electron microscopy),



Scheme 1. Formation of micron-scale corrals with hydrophobic alkanethiolate bottoms and walls consisting of a hydrophilic three-layer poly(acrylic acid)/poly(ethylene glycol) nanocomposite.

an evaporated gold substrate is patterned with a hexadecanethiol (C16SH) SAM by soft lithography.^[13] Second, the unmodified regions of the gold substrate are filled with a SAM of 11-sulfanylundecanoic acid (also called mercaptoundecanoic acid, MUA). Next, the terminal acid groups of the MUA-patterned portions of the mixed monolayer are activated and treated with α,ω -diamino-substituted poly(*tert*-butyl acrylate) ($\text{H}_2\text{NR-PTBA-RNH}_2$) to yield the amide-grafted polymer layer. Hydrolysis of PTBA with MeSO_3H yields the first layer of PAA, and two additional cycles of activation, grafting, and hydrolysis yields a hyperbranched

[*] Prof. R. M. Crooks, Dr. P. Ghosh, Dr. W. M. Lackowski
Department of Chemistry
Texas A&M University
P.O. Box 30012, College Station, TX 77842–3012 (USA)
Fax: (+1) 409-845-1399
E-mail: crooks@tamu.edu

M. L. Amirpour, Prof. M. V. Pishko
Department of Chemical Engineering, Texas A&M University
College Station, TX 77843–3122 (USA)

[**] This work was supported by the National Science Foundation (CHE-9313441), the Robert A. Welch Foundation, and the State of Texas Higher Education Coordinating Board through the Advanced Technology Program (010366-096) and the Advanced Research Program at Texas A&M University. We thank Prof. David E. Bergbreiter and his research group at Texas A&M University for helpful comments and for providing the α,ω -diamino poly(*tert*-butylacrylate). We also thank Dr. Li Sun (Texas A&M University) for help with the lithography experiments.